

Supplementary Information

Generation of homogeneous midbrain organoids with in vivo–like cellular composition facilitates neurotoxin-based Parkinson’s disease modeling

Tae Hwan Kwak, Ji Hyun Kang, Sai Hali, Jonghun Kim, Kee-Pyo Kim, Chanhyeok Park, Ju-Hyun Lee, Ha Kyun Ryu, Ji Eun Na, Junghyun Jo, Hyunsoo Shawn Je, Huck-Hui Ng, Jeongwoo Kwon, Nam-Hyung Kim, Kwon Ho Hong, Woong Sun, Chi Hye Chung, Im Joo Rhyu, and Dong Wook Han

Supplementary Figures

Supplementary Fig. 1, Supplementary Fig. 2, Supplementary Fig. 3, Supplementary Fig. 4, Supplementary Fig. 5, Supplementary Fig. 6, Supplementary Fig. 7

Supplementary Table

Supplementary Table 1

Information of Supplementary Video

Supplementary Video 1

Supplementary Methods

Supplementary Figures

Figure S1

Figure Supplementary 1

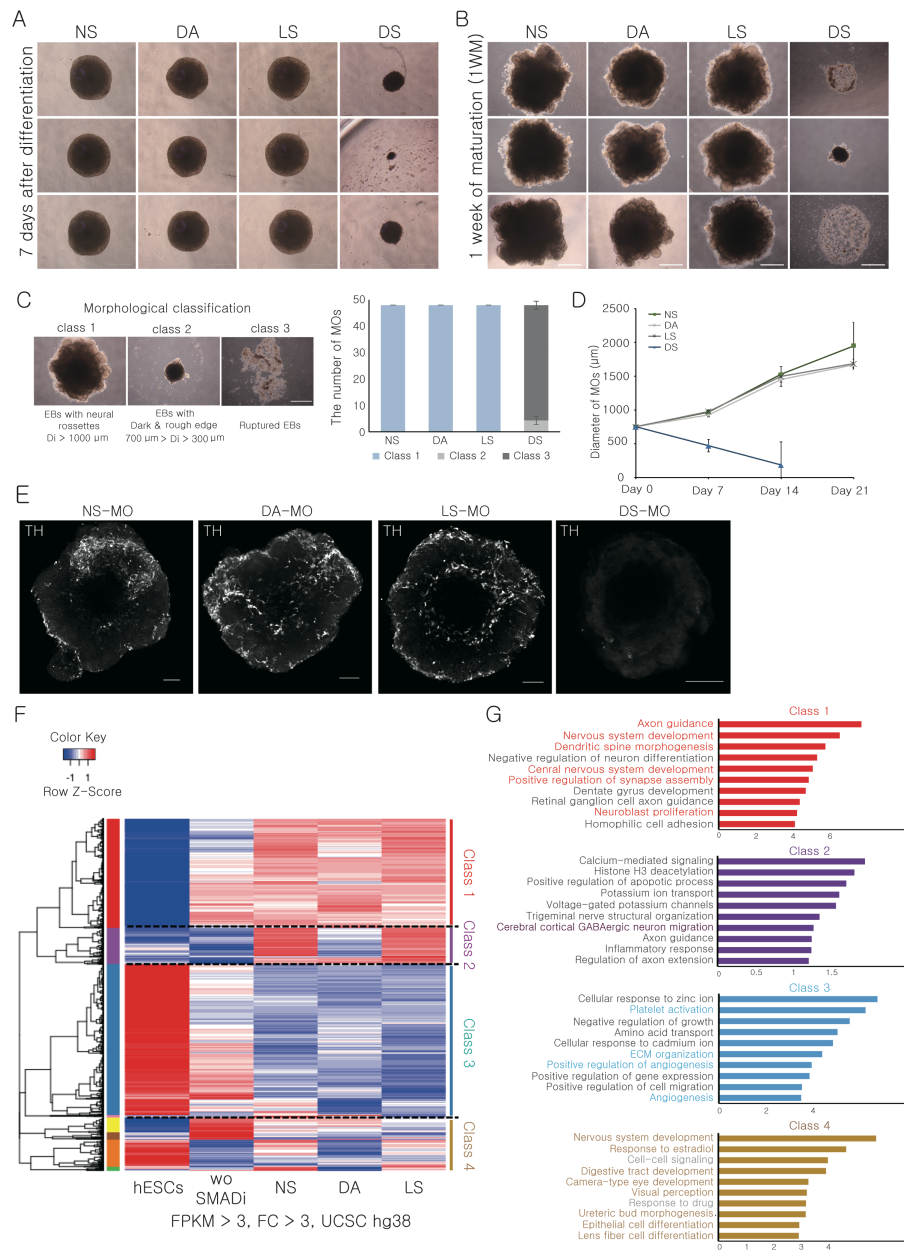


Figure S1. Generation of MOs with distinct combinations of dual SMAD inhibitors.

(A and B) Representative morphology of EBs on day 7 of differentiation (A) and MOs after 1WM (B). Scale bar, 500 μm.

(C) Number and quality of MOs (1WM) generated from distinct combinations of dual SMAD inhibitors. Data are presented as mean ± SD from three independent experiments. Scale bar, 500 μm.

(D) Average diameter of NS-, DA-, LS-, and DS-MOs was measured in a time-course manner. Data are presented as mean \pm SD of triplicate values.

(E) Representative section image of whole mount confocal microscopy displaying distribution of mDA neurons expressing TH in NS-, DA-, LS-, and DS-MOs. Scale bar, 200 μ m.

(F) Heatmap representing the global gene expression profile of day-7 EBs generated with distinct combinations of dual SMAD inhibitors. The red-blue color scale is the normalized expression value, denoted as the row Z-score. Red and blue colors indicate increased expression and decreased expression, respectively. Differentially expressed genes among each sample are categorized into four groups (class 1 to 4).

(G) GO enrichment analysis based on the gene set highly enriched in each group (class 1 to 4).

Figure S2

Figure Supplementary 2

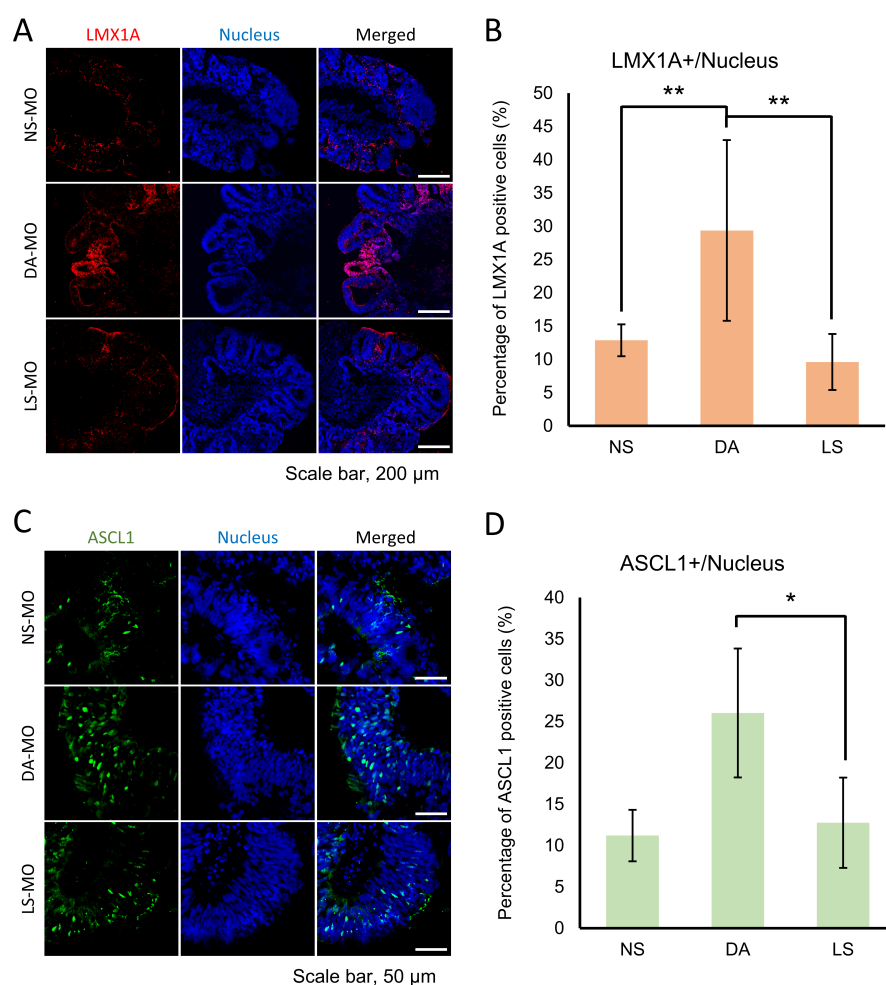


Figure S2. Midbrain-specific regional identity of DA-MOs

(A) Confocal images showing distribution of midbrain specific progenitors expressing both LMX1A in MOs grown under distinct conditions (NS-, DA-, and LS-MOs) after 4WM. Scale bar, 200 μ m.

(B) Percentage of LMX1A-positive midbrain specific progenitors. Data are presented as mean \pm SD from three independent experiments. n = 6–8 organoids per group; **p < 0.01.

(C) Confocal images showing distribution of mDA neuronal progenitors expressing both LMX1A in MOs grown under distinct conditions (NS-, DA-, and LS-MOs) after 4WM. Scale bar, 50 μ m.

(D) Percentage of LMX1A-positive mDA neuronal progenitors. Data are presented as mean \pm SD from three independent experiments. n = 6–8 organoids per group; *p < 0.05.

Figure S3

Supplementary figure 3

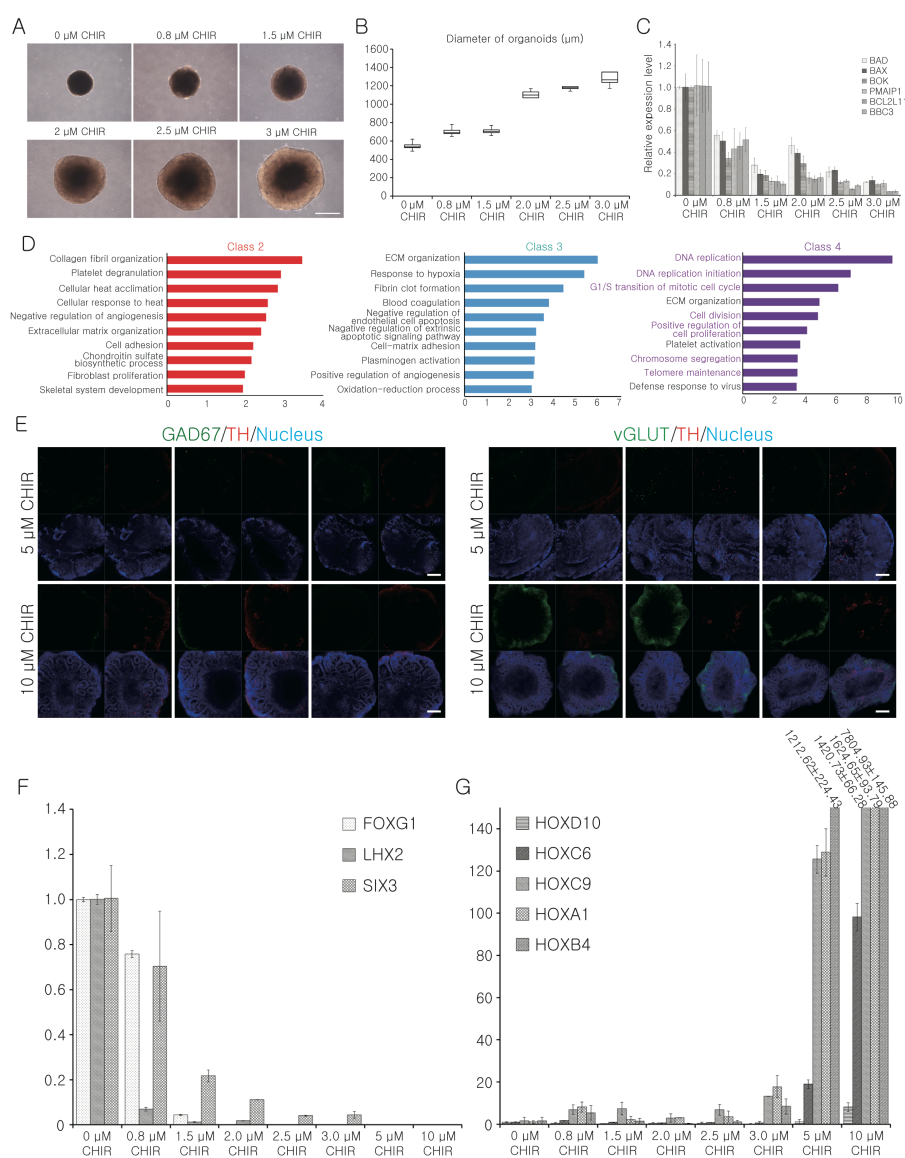


Figure S3. Generation of homogeneous MOs using an *in vitro* WNT gradient.

(A and B) Representative morphology (A) and average diameter (B) of MOs generated by an *in vitro* WNT gradient (1WM). Data are presented as mean \pm SD of triplicate values. Scale bar, 500 μ m.

(C) Expression of pro-apoptotic genes was analyzed by qPCR using MOs generated by the *in vitro* WNT gradient (1WM). Expression levels are normalized to those of MOs with 0 μ M CHIR99021. Data are presented as mean \pm SD of triplicate values.

(D) GO enrichment analysis based on the gene set highly enriched in classes 2, 3, and 4, which are categorized in Fig 3B.

(E) Representative section images of whole mount confocal microscopy displaying the distribution of TH-positive mDA neurons in DA-MOs (3WM) with higher concentrations of CHIR99021 (5 and 10 μ M). Scale bar, 200 μ m.

(F and G) Expression of forebrain- **(F)** and spinal cord-specific markers **(G)** was analyzed by qPCR using DA-MOs produced by the *in vitro* WNT gradient (3WM). Expression levels are normalized to those of MOs with 0 μ M CHIR99021. Data are presented as mean \pm SD of triplicate values.

Figure S4

Figure Supplementary 4

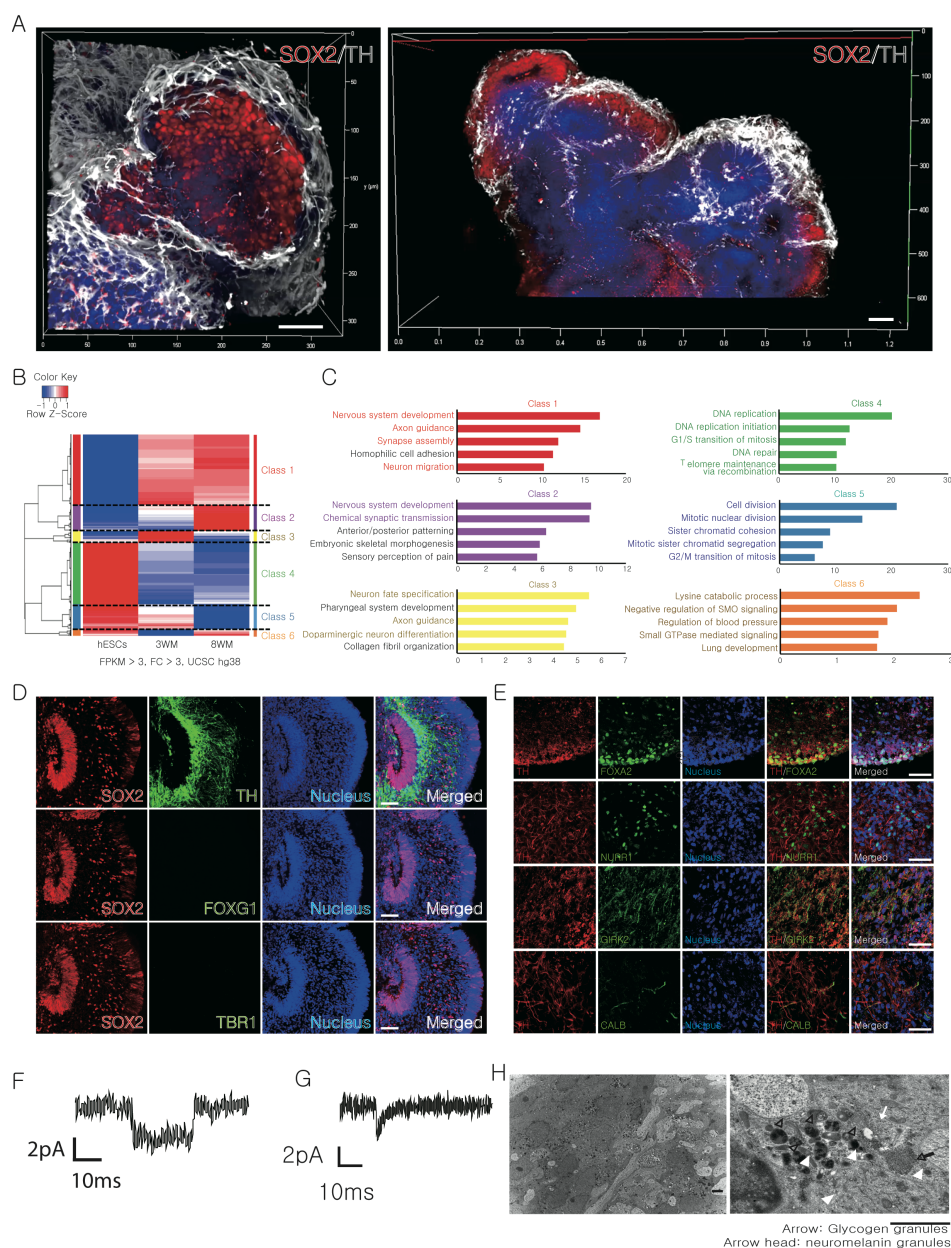


Figure S4. Characterization of DAC3.0 MOs.

(A) 3D reconstructed confocal images showing laminated structure of DAC3.0 MOs (4WM). Scale bar, 50 μ m.

(B) Heatmap displaying the global gene expression profile of DAC3.0 MOs (3WM and 8WM). The red-blue color scale is the normalized expression value, denoted as the row Z-score. Red and blue colors indicate increased expression and decreased expression, respectively. Differentially expressed genes among each sample are categorized into six groups (class 1 to 6).

(C) GO enrichment analysis based on the gene set highly enriched in each group (class 1 to 6).

(D) Representative images of single neural lobe immunostained with SOX2, TH, FOXG1, and TBR1 in DAC3.0 MOs (4WM). Scale bar, 100 μ m.

(E) Confocal images displaying mDA neurons expressing FOXA2, NURR1, GIRK2, and Calbindin in DAC3.0 MOs (8WM). Scale bar, 50 μ m.

(F and G) Ion channel activity (F) and spontaneous synaptic activity (G) were recorded in DAC3.0 MOs (8WM).

(H) TEM images displaying neuromelanin-like granules in mDA neurons (arrows) and glycogen granules in astrocytes (arrowheads) contained within DAC3.0 MOs (12WM). Scale bar, 2 μ m.

Figure S5

Figure Supplementary 5

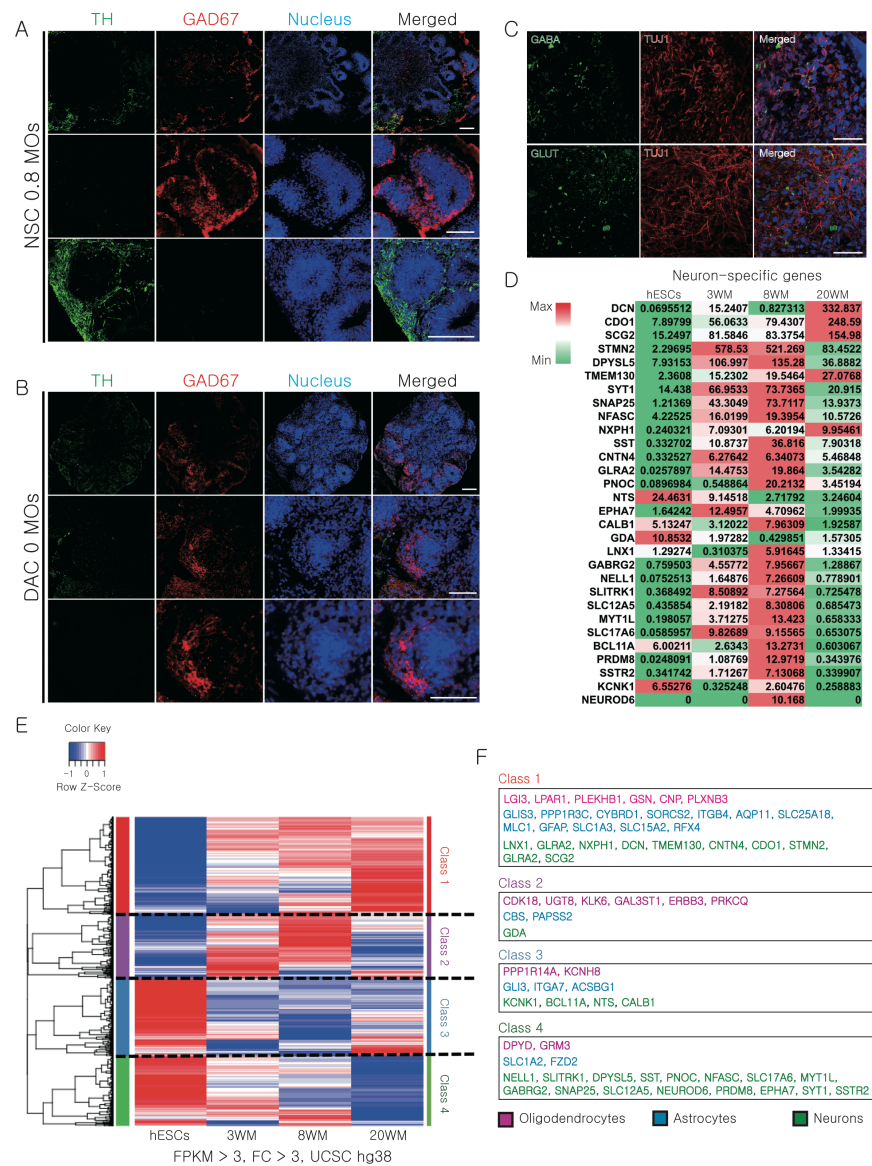


Figure S5. Cell type diversity in DAC3.0 MOs.

(A and B) Confocal images representing the distribution of TH-positive mDA neurons and GAD67-positive GABAergic neurons in NSC0.8 MOs (A) and DAC0 MOs (B) (8WM). Scale Bar, 100 μ m.

(C) Confocal images displaying GABA-positive GABAergic neurons and GLUT-positive glutamatergic neurons in DAC3.0 MOs (8WM). Scale bar, 50 μ m.

(D) Heatmap representing the expression patterns of markers related to neurons in DAC3.0 MOs (3WM, 8WM, and 20WM). Color bar at the left top indicates gene expression in \log_2 scale. Red and green colors represent higher and lower expression levels, respectively.

(E) Heatmap displaying the global gene expression profile of DAC3.0 MOs (3WM, 8WM, and 20WM). The red-blue color scale is the normalized expression value, denoted as the row Z-score. Red and blue colors indicate increased expression and decreased expression, respectively. Differentially expressed genes among each sample are categorized into four groups (class 1 to 4).

(F) Distribution of cell type-specific marker genes (oligodendrocyte-, astrocyte-, and neuron-specific genes) in distinct gene categories (class 1 to 4).

Figure S6

Figure Supplementary 6

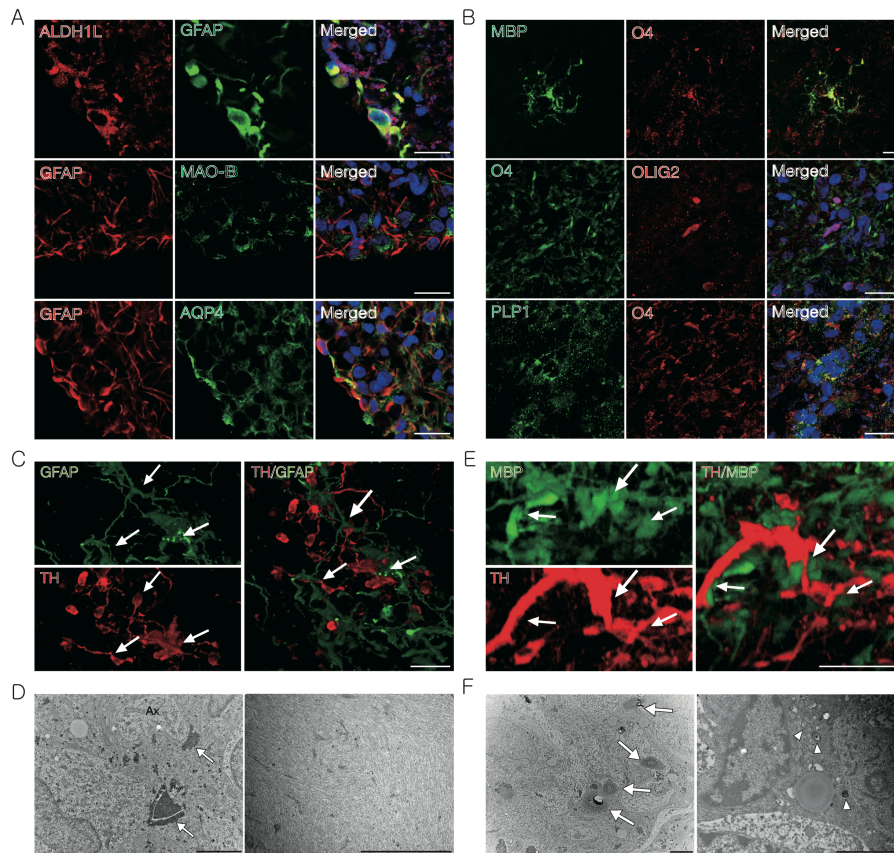


Figure S6. Gliogenesis in DAC3.0 MOs.

(A and B) Expression of functional markers of astrocytes (A) and oligodendrocytes (B) in DAC3.0 MOs (12WM). Scale bar, 25 μ m.

(C) 3D reconstructed Z-stacks showing direct connection between GFAP-positive astrocytes and TH-positive DA neurons. Scale bar, 50 μ m.

(D) TEM images displaying glycogen granule-containing (arrows) astrocytes surrounding neuronal axon (Ax) (left panel) and glial filament-like structure (right panel). Scale bar, 2 μ m.

(E) 3D reconstructed Z-stacks displaying direct connection between MBP-positive oligodendrocytes and TH-positive DA neurons. Scale bar, 50 μ m.

(F) TEM images showing global distribution of myelinating oligodendrocytes (arrows) in DAC3.0 MOs (left panel). Oligodendrocyte-like cell body (right panel) containing a dark nucleus with clumped chromatin and myelin-like inclusions (arrow heads). Scale bar, 2 μ m.

Figure S7

Figure Supplementary 7

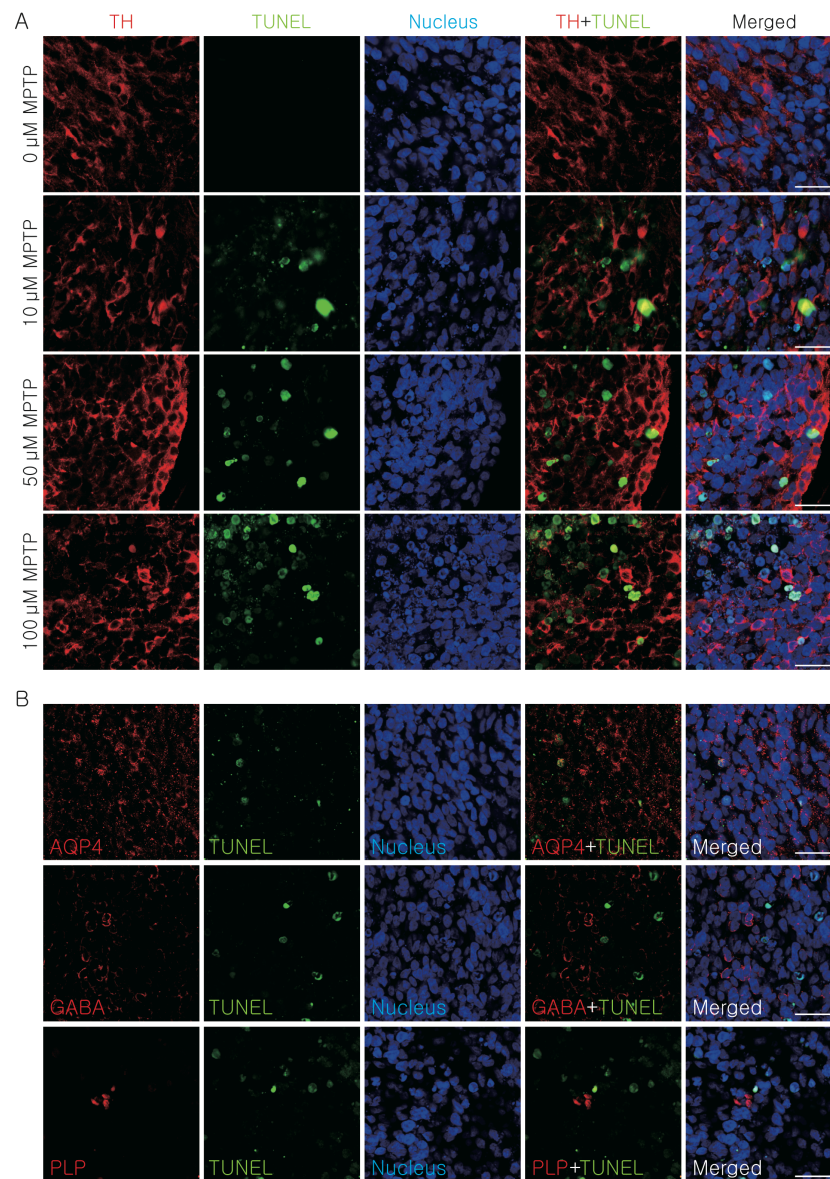


Figure S7. mDA neuron-specific cell death in MPTP-treated DAC3.0 MOs.

(A) TUNEL-labeled mDA neurons in MPTP-treated DAC3.0 MOs (0, 10, 50, and 100 μ M). Scale bar, 25 μ m.

(B) mDA neuron-specific cell death—no cell death of other cell types such as GABAergic neurons (GABA), astrocytes (AQP4), and oligodendrocytes (PLP)—in MPTP-treated DAC3.0 MOs. Scale bar, 25 μ m.

Supplementary Table

Supplementary Table 1. Primers used for qPCR

Gene Name	Genebank Number	Primer sequence
<i>NANOG</i>	AB093576.1	TGCAACCTGAAGACGTGTGA CTATGAGGGATGGGAGGA
<i>OCT4</i>	BC117435.1	GACAGGGGGAGGGGAGGAGCTAGG CTTCCCTCCAACCAGTTGCCCCAAAC
<i>SOX2</i>	BC013923.2	AGACTGCACATGAGCCAGCA CGTCTCCAGCCAGCTTCAAC
<i>N-CAD</i>	AF006514.1	TGATGAAGAAGGTGGAGGAGAAGA ATTCGTCGGATTCCCACAGG
<i>OTX2</i>	AB593058.1	CCCTCACTCGCCACATCTAC GTTCAGAGTCTCTTGGTGGGT
<i>PLZF</i>	NM_006006.5	TCCCGCCCGACTGGAGGATA TTCTTTTCTGGCTCCCCGCTC
<i>EOMES</i>	AB031038.1	CTCAAAAGGCATGGGAGGGTA CACCACCAAGTCCATCTGCAA
<i>SOX17</i>	AB073988.1	CCTTAGCTCCAGGAAGTGTG GCCAGCTCCGCGGTATATTACT
<i>T</i>	BC098425.1	CGCCTCATAGCCTCATGGAC CACTGGCTGCCACGACAAA
<i>BOK</i>	AF089746.1	GCTGGCCACATCTTCTCTGC TGCTGACCACACACTTGAGGAC
<i>BAX</i>	NM_007527	TGCTGACGTGGACACGGACT CCAGCCACCCTGGTCTTGGA
<i>BAD</i>	NM_007522	TCGGAGTCGCCACAGTTCGT GCGCTCTTTGGGCGAGGAAG
<i>PMAIP1</i>	KU178264.1	GGGAAGAAGGCGCGCAAGAA AGTTTCTGCCGGAAGTTCAGTTTGT
<i>BCL2L11</i>	NM_138621.5	GCCCAAGAGTTGCGGCGTATT TCTCCACACCAGGCGGACAAT
<i>BBC3</i>	U82987.1	CGGACGACCTCAACGCACAGTA AAGGGCAGGAGTCCCATGATGA
<i>FOXG1</i>	BC050072	GCGGGCCAGACCAGTTACTT CCCAGACAGTCCCGTCGTAA
<i>LHX2</i>	AF124735.1	ACTTCTGTGCCTGGCAACCTG TCTGTTTCCAGGCGAGATCCT
<i>SIX3</i>	AF049339.1	AACCTCCAGCGACTCGGAAT TTCGGTTTGTCTGGGGATG
<i>LRTM1</i>	BC040732.1	CTGCCATGCCCTTCGTGTGT AACACTTGTCGGGCAGCTG
<i>DAT</i>	NM_001044.5	CGCCACTGGCTCAAGGTGTA CCGGCACGGAAAGGTGTAA
<i>TH</i>	NM_199292.2	CTGAGATTTCGGGCCTTCGAC TGCACCTAGCCAATGGCACT
<i>LMX1B</i>	AH006310.2	GGCATCAAGATGGAGGAGCA TGGTGAGGGCTTGCTGACAC
<i>LMX1A</i>	NM_177398.4	AAAGCGCGATCGACACCTC TCCCGGTAGAAGCAGGTGGT
<i>ASCL1</i>	NM_004316.4	GGTGATCGCACAACCTGCAT GTTCTGAGCGCTTCCCGTTT
<i>PAX3</i>	NM_181457.3	TTTCCGTTTCGCCTTCACCT ACGATCTTGTGGCGGATGTG
<i>HOXD10</i>	NM_002148.3	CTAATTCCAGCGTTTGGTGC CTGAGGTCTCCGTGTCCAGT
<i>HOXC6</i>	CR456954.1	GAATGAGGGAAGACGAGAAAGAG CATAGGCGGTGGAATTGAGG
<i>HOXC9</i>	AH010088.2	CTCCTAGCGTCCAGGTTTCC CGGGTGATATACCACGGACG
<i>HOXA1</i>	U10421.1	AAATCAGGAAGCAGACCCAC GTAGCCGTACTCTCCAACCTTC
<i>HOXB4</i>	AF307160.1	TACCCCTGGATGCGCAAAGTTC TGGTGTGGGCAACTTGTGG

Supplementary Video

Supplementary Video 1. The laminated layer structure of midbrain-like neural lobe in DAC3.0 MOs

The video showing three-dimensionally reconstructed layer structure of midbrain-like neural lobe in DAC3.0 MOs. The white and red color marked TH-positive mDA neurons and SOX2-positive neural progenitor respectively. The nucleus was counter-stained with TOPRO-3 (blue color).

Supplementary Methods

Cell culture

hESCs were maintained in TeSRTM-E8TM medium (STEMCELL Technologies). For passaging hESCs, ReLeSRTM (STEMCELL Technologies) was used according to the manufacturer's instructions.

Generation of midbrain organoids

To generate MOs, hESCs were dissociated into single cells using TrypLETM (Gibco), and 1.0×10^4 single cell–dissociated hESCs were replated per well in ultra low–attachment U-bottom 96-well plates (Corning) for the generation of uniform EBs using embryoid body forming medium (EBM), consisting of DMEM/F12 (Corning) supplemented with 20% KSR (Gibco), 1% penicillin/streptomycin (PS) (Gibco), GlutaMAXTM (Gibco), NEAA (Gibco), 55 μ M β -mercaptoethanol (Gibco), 1 μ g/ml of heparin (Sigma), 3% fetal bovine serum (FBS) (Seradigm), 4 ng/ml of bFGF (Peprotech), and 50 μ M Y27632 (Calbiochem). At 24 hrs after plating, the medium was changed to brain organoid generation medium (BGM) containing of 1:1 mix of DMEM/F12 (Corning) and Neurobasal Medium (Gibco) supplemented with 100x N2 supplement (Gibco), 50x B27 without vitamin A (Gibco), 1% penicillin/streptomycin (PS) (Gibco), 1% GlutaMAXTM (Gibco), 1% NEAA (Gibco), 55 μ M β -mercaptoethanol (Gibco), and 1 μ g/ml heparin (Sigma). For mesencephalon specification, distinct combinations of dual SMAD inhibitors employed in previous studies were used: 200 ng/ml Noggin (Peprotech) + 10 μ M SB431542 (Peprotech)¹; 2 μ M dorsomorphin (Sigma) + 2 μ M A83-01 (Peprotech)²; 100 nM LDN (Biogems) + 10 μ M SB431542 (Peprotech)²; and 10 μ M dorsomorphin (Sigma) + 10 μ M SB431542 (Peprotech)³. To create an *in vitro* WNT gradient, different concentrations of CHIR99021 (0, 0.8, 1.5, 2, 2.5, 3, 5, and 10 μ M) (Tocris) were used in the presence of 1 μ M IWP2 (Biogems). On day 4, 100 ng/ml FGF8 (Peprotech) and 2 μ M SAG (Peprotech) were added to induce specification into the mesencephalic floor plate. After 3 days, MOs were embedded into growth factor–reduced matrigel (Corning) droplets. Matrigel-embedded MOs were transferred onto 6-cm petri dishes containing BGM supplemented with 100 ng/ml of FGF8, 2 μ M SAG, 200 ng/ml laminin (BD science), and 2.5 μ g/ml insulin (Thermo) for facilitating basal-apical lamination. After 2 days, MOs were transferred into ultra low–attachment 6-well plates (Corning) containing brain organoid maturation medium (BMM), consisting of 1:1 mix of DMEM/F12 (Corning) and Neurobasal Medium (Gibco) supplemented with 100x N2 supplement (Gibco), 50x B27 (Gibco), 1% penicillin/streptomycin (PS) (Gibco), 1% GlutaMAXTM

(Gibco), 1% NEAA (Gibco), 55 μ M β -mercaptoethanol (Gibco), 1 μ g/ml heparin (Sigma), 10 ng/ml BDNF (Peprotech), 10 ng/ml GDNF (Peprotech), 200 μ M ascorbic acid (Peprotech), and 125 μ M cAMP (Peprotech). From this maturation step, MOs were cultured on an orbital shaker (Stuart). BMM was replaced every other day. For assessing the production of neuromelanin in MOs, 50 μ M DA (Sigma) was added to BMM from 8WM MOs.

Generation of cerebral organoids

To generate cerebral organoids (COs), 1×10^4 single cell–dissociated hESCs were plated on each well of ultra low–attachment U-bottom 96-well plates (Corning). At 24hrs after plating, BGM supplemented with 2 μ M dorsomorphin and 2 μ M A83-01 was added to EBs. The medium was replaced every other day. After 7 days of differentiation, COs were embedded into growth factor–reduced matrigel (Corning) droplets. Matrigel-embedded COs were transferred to 6-cm petri dishes containing BGM supplemented with 200 ng/ml laminin and 2.5 μ g/ml insulin for inducing basal-apical lamination. After 2 days, COs were transferred into ultra low–attachment 6-well plates (Corning) containing BMM and cultured on an orbital shaker (Stuart). The culture medium was replaced every other day.

Gene expression analysis

For comparing the relative expression levels of marker genes, total RNA was isolated from organoids using the Hybrid-RTM RNA isolation kit (GeneAll). Complementary DNA (cDNA) was synthesized with the High Capacity cDNA Reverse Transcription kit (Applied biosystems) using 1 μ g of isolated total RNA. Quantitative RT-PCR (qPCR) was performed with the SYBR green PCR Master Mix (Applied biosystems) using the ABI 7500 real-time PCR system (Applied biosystems). Δ Ct values were calculated by subtracting the Gapdh Ct value from that of each target gene. Relative expression levels were calculated by using $2^{-\Delta\Delta Ct}$ methods. Primer sequences used for qPCR are listed in supplementary Table S1.

Cryosection

The organoids were fixed with 4% paraformaldehyde (Sigma) for 15 to 20 min at room temperature and washed three times with PBS. The fixed organoids were transferred to 30% sucrose solution and incubated at 4°C until

the organoids sank to the bottom. Equilibrated organoids were then transferred to freezing mold containing 1:1 mixture of OCT compound and 30% sucrose solution and slowly frozen on dry ice. Frozen blocks can be stored at -80 °C for up to 2 months. Frozen blocks containing organoids were sliced with a cryotome. The microsections of frozen blocks were attached onto silane-coated glass microslides (Muto pure chemical). Sliced tissue sections were air dried.

Immunohistochemistry

Immunohistochemical analysis was performed on the sectioned organoids. Briefly, the dried tissue sections were permeabilized and blocked with DPBS (Welgene) containing 0.03% Triton X-100 (Sigma) and 5% FBS (Seradigm) for 1 hr at room temperature. The permeabilized tissue sections were then incubated with the appropriate primary antibody for 16 hrs at 4°C, and then incubated with the appropriate secondary antibody after being washed three times with DPBS (Welgene). Counterstaining was performed with TOPRO-3 (Life Technology). Primary antibodies used for immunohistochemistry are as follows: MAP2 (Merck millipore), TH (Abcam), ASCL1 (BD pharmingen), LMX1A (Santa cruz), TBR1 (Abcam), TUJ1 (Biolegend), SOX2 (R&D system), GAD67 (Merck millipore), vGLUT (Merck millipore), FOXA2 (Abcam), LRTM1 (Cusabio), DAT (Merck millipore), NURR1 (Santa cruz), GIRK2 (Abcam), CALB (Merck millipore), FOXG1 (Abcam), GABA (Sigma), GLUT (Cusabio), GFAP (CiteAb), S100B (Abcam), MBP (Abcam), ALDH1L (Abcam), MAO-B (Abcam), AQP4 (Merck millipore), O4 (R&D system), OLIG2 (Merck millipore), PLP1 (Cusabio), and Caspase-3 (Cell signaling).

Whole mount immunostaining

For immunostaining of whole organoids without microsectioning, whole organoids were fixed with 4% paraformaldehyde (Sigma) for 15 to 20 min at room temperature and washed three times with PBST containing DPBS supplemented with 0.1% Triton X-100. Fixed organoids were transferred into blocking solution containing DPBS supplemented with 6% BSA (Sigma), 0.2% Triton X-100, and 0.01% sodium azide (Biosolution) and then incubated overnight on rocking platform mixer at room temperature. The samples were incubated with primary antibodies for 48 hrs on a rocking platform mixer at room temperature. After washing three times with PBST, the organoids were incubated with fluorescence-labeled secondary antibody and

TOPRO-3 on a rocking platform mixer for 48 hrs at room temperature. After rinsing three times with PBST, the immunostained organoids were transferred onto 35-mm glass-bottom dishes (SPL) and immersed into clearing solution to adjust the RI value. For whole mount confocal imaging, LSM 710 (Zeiss) was used.

Fontana-Masson staining

The neuromelanin pigment was stained by the Fontana-Masson Stain Kit (Abcam) according to manufacturer's instructions using cryosectioned organoids.

TEM imaging

The organoids were pretreated with 0.1 M phosphate buffer (pH 7.4) containing 2% paraformaldehyde and 2.5% glutaraldehyde for 16 hrs at 4°C. The organoids were then fixed with 1% osmium tetroxide for 90 min. The fixed organoids were dehydrated by stepwise immersion in 60%, 70%, 80%, and 90% ethanol, for 20 min each time. The organoids were completely dehydrated by immersing them three times in 100% ethanol for 90 min for each time. The dehydrated organoids were embedded into Epon and allowed to polymerize at 68°C for 48 hrs to form a block. The block was sliced into 60-nm thin sections by using a UC6 ultramicrotome (Leica microsystems). The section slices were stained with uranyl acetate and lead citrate and observed by the transmission electron microscope (TEM) H-7500 (Hitachi).

Electrophysiology

To examine the electrophysiological properties of organoids, whole cell patch clamp recording was performed using a MultiClamp 700B amplifier that was filtered 5 kHz and sampled at 10 kHz. An organoid was placed in a chamber and submerged into continuously perfused artificial CSF containing 1 mM NaH_2PO_4 , 26.2 mM NaHCO_3 , 118 mM NaCl , 2.5 mM KCl , 11 mM Glucose, 4 mM CaCl_2 , and 1 mM MgCl_2 that was bubbled with 95% O_2 and 5% CO_2 . An organoid was visualized using upright microscope BX51WI (Olympus) equipped with a 40x water-immersion lens. Recording pipettes with resistances of 3-6 M Ω were filled with internal solution containing 135 mM K-gluconate, 10 mM KCl , 10 mM HEPES, 1 mM EGTA, and 2 mM Na_2ATP . The pH was adjusted to 7.2-7.4 with KOH. Data was acquired using clampex 10.3 software (Molecular devices). Resting membrane potentials were measured in a current-clamp configuration with a holding current of 0 pA. Action

potentials of neurons in organoids were elicited by injecting a series of current steps (0 to 100 pA, with 10 pA increments, 200 ms long). Spontaneous postsynaptic currents and single-channel activities were recorded in a voltage clamp configuration while holding the membrane potential at -70 mV.

Bioinformatics analysis

RNA-seq data paired-end files were mapped to the human genome (UCSC, hg38) build using the RNA-seq aligner STAR (v2.5.2b). After mapping, the gene expression level was calculated as Fragments Per Kilobase Million (FPKM) by Cufflinks, the transcriptome assembly and differential expression analysis tool (v2.2.1), based on the default options. To determine clustering in gene expression, statistical analyses were executed with the heatmap.2 function (gplots package) in the statistical software R (v3.3.2). Analysis of functional Gene Ontology (GO) was performed based on differentially expressed genes by using DAVID (Database for Annotation, Visualization and Integrated Discovery, v6.8). In addition, RNA-seq reads mapped by hg38 were visualized by the processing tool IGV (Integrative Genomics Viewer).

TUNEL assay

To observe apoptotic cells in organoids, the TUNEL assay was performed using the *in situ* cell-death detection kit, fluorescein (Roche) according to manufacturer's protocol. Briefly, the micro-sectioned organoids on glass slides were prepared for the TUNEL assay. Samples were permeabilized with permeabilization solution for 2 min on ice and washed three times with PBS. The samples were then placed in citrate buffer, received 750 W microwave irradiation for 1 min, and then were translocated to cool distilled water. Samples were immersed for 30 min in Tris-HCl (0.1 M, pH 7.5), containing 3% BSA and 20% normal bovine serum at room temperature. Then, the TUNEL reaction mixture was added on the tissue section. After the TUNNEL assay, organoid sections were blocked and co-stained with antibody raised against TH (Abcam), GABA (Sigma), AQP4 (Merck millipore), and PLP1 (Cusabio).

Statistical analysis

For statistical analysis, the unpaired t-test and ANOVA were used for calculating p values. All the values were calculated from at least triplicate experiments and the p values were presented as * $P < 0.05$; ** $P < 0.01$; and *** $P < 0.001$.

Reference

1. Jo J, Xiao Y, Sun AX, et al. Midbrain-like Organoids from Human Pluripotent Stem Cells Contain Functional Dopaminergic and Neuromelanin-Producing Neurons. *Cell Stem Cell*. 2016;19:248-257.
2. Qian X, Nguyen HN, Song MM, et al. Brain-Region-Specific Organoids Using Mini-bioreactors for Modeling ZIKV Exposure. *Cell*. 2016;165:1238-1254.
3. Moya N, Cutts J, Gaasterland T, et al. Endogenous WNT signaling regulates hPSC-derived neural progenitor cell heterogeneity and specifies their regional identity. *Stem Cell Reports*. 2014;3:1015-1028.